

## The TAOS Project Stellar Variability II. Detection of 15 Variable Stars

S. Mondal<sup>1,2</sup>, C.C. Lin<sup>1</sup>, W. P. Chen<sup>1</sup>, Z.-W. Zhang<sup>1</sup>, C. Alcock<sup>3</sup>, T. Axelrod<sup>4</sup>, F. B. Bianco<sup>3,5,6,7</sup>, Y.-I. Byun<sup>8</sup>, N. K. Coehlo<sup>9</sup>, K. H. Cook<sup>10</sup>, R. Dave<sup>11</sup>, D.-W. Kim<sup>8</sup>, S.-K. King<sup>12</sup>, T. Lee<sup>12</sup>, M. J. Lehner<sup>12,5,3</sup>, H.-C. Lin<sup>1</sup>, S. L. Marshall<sup>13,10</sup>, P. Protopapas<sup>11,3</sup>, J. A. Rice<sup>9</sup>, M. E. Schwamb<sup>14</sup>, J.-H. Wang<sup>1,12</sup>, S.-Y. Wang<sup>12</sup> and C.-Y. Wen<sup>12</sup>

soumen@aries.res.in

### ABSTRACT

The Taiwanese-American Occultation Survey (TAOS) project has collected more than a billion photometric measurements since 2005 January. These sky survey data—covering timescales from a fraction of a second to a few hundred days—are a useful source to study stellar variability. A total of 167 star fields, mostly along the ecliptic plane, have been selected for photometric monitoring with the TAOS telescopes. This paper presents our initial analysis of a search for periodic variable stars from the time-series TAOS data on one particular TAOS field, No. 151 (RA = 17<sup>h</sup>30<sup>m</sup>6<sup>s</sup>.67, Dec = 27°17′30″, J2000), which had been observed over 47 epochs in 2005. A total of 81 candidate variables are identified in the 3 square degree field, with magnitudes in the range  $8 < R < 16$ . On the basis of the periodicity and shape of the lightcurves, 29

---

<sup>1</sup>Institute of Astronomy, National Central University, 300 Jhongda Rd, Jhongli 32054, Taiwan

<sup>2</sup>Aryabhata Research Institute of Observational Sciences, Manora Peak, Nainital-263129, India

<sup>3</sup>Harvard-Smithsonian Center for Astrophysics, 60 Garden Street, Cambridge, MA 02138

<sup>4</sup>Steward Observatory, 933 North Cherry Avenue, Room N204 Tucson AZ 85721

<sup>5</sup>Department of Physics and Astronomy, University of Pennsylvania, 209 South 33rd Street, Philadelphia, PA 19104

<sup>6</sup>Department of Physics, University of California Santa Barbara, Mail Code 9530, Santa Barbara CA 93106-9530

<sup>7</sup>Las Cumbres Observatory Global Telescope Network, Inc. 6740 Cortona Dr. Suite 102, Santa Barbara, CA 93117

<sup>8</sup>Department of Astronomy, Yonsei University, 134 Shinchon, Seoul 120-749, Korea

<sup>9</sup>Department of Statistics, University of California Berkeley, 367 Evans Hall, Berkeley, CA 94720

<sup>10</sup>Institute for Geophysics and Planetary Physics, Lawrence Livermore National Laboratory, Livermore, CA 94550

<sup>11</sup>Initiative in Innovative Computing at Harvard, 120 Oxford St., Cambridge MA 02138

<sup>12</sup>Institute of Astronomy and Astrophysics, Academia Sinica. P.O. Box 23-141, Taipei 106, Taiwan

<sup>13</sup>Kavli Institute for Particle Astrophysics and Cosmology, 2575 Sand Hill Road, MS 29, Menlo Park, CA 94025

<sup>14</sup>Division of Geological and Planetary Sciences, California Institute of Technology, 1201 E. California Blvd., Pasadena, CA 91125

variables, 15 of which were previously unknown, are classified as RR Lyrae, Cepheid,  $\delta$  Scuti, SX Phonencis, semi-regular and eclipsing binaries.

*Subject headings:* stars: variables: Cepheids— stars: variables: delta Scuti— stars: variables: general— stars: variables: RR Lyraes

## 1. Introduction

The Taiwanese-American Occultation Survey (TAOS) project aims to search for stellar occultation by small ( $\sim 1$  km diameter) *Kuiper Belt Objects* (KBOs). The KBO population consists of remnant planetesimals in our Solar System, which typically have low to intermediate (below  $30^\circ$ ) inclination orbits and heliocentric distances between 30 and 50 AU (Edgeworth 1949; Kuiper 1951; Morbidelli & Levison 2003). The size distribution of large KBOs shows a broken power law with the break occurring  $\sim 30$ – $100$  km that indicates a relative deficiency of small KBOs. Such a broken power law is believed to be the consequence of competing processes of agglomeration to form progressively larger bodies versus collisional destruction. The size distribution thus provides critical information of the dynamical history of the Solar System. The stellar occultation technique, namely the dimming of a background star by a passing KBO, is the only technique capable of detecting cometary-sized bodies, which are too faint for direct imaging even with the largest telescopes (Alcock et al. 2003; Zhang et al. 2008). So far, TAOS has collected several billion stellar photometric measurements, and no occultation events have been detected, indicating a significant depletion of small KBOs (Zhang et al. 2008; Bianco et al. 2010).

Several projects have discovered numerous variable stars as byproducts, for instance the MA-CHO (Alcock et al. 1995, 1998), EROS (Beaulieu et al. 1995; Derue et al. 2002), OGLE (Cieslinski et al. 2003; Wray & Paczynski 2004), and ROTSE-I (Akerlof et al. 2000; Kinemuchi et al. 2006; Hoffman, Harrison & Mo 2009). Such data have enriched our knowledge of stellar variability in the Galactic fields and the Magellanic Clouds, which not only improves the number statistics, but also has helped to shed light on the detailed mechanisms of stellar variability. Knowledge of the variability has been so far still relatively poor for even the bright stars. Recent large-area sky survey projects, however, have started to turn up large numbers of variable stars. These projects include the All Sky Automated Survey (Pojamanski, Pilecki & Szczygiel 2005, ASAS), the observations by the Hungarian Automated Telescope (Bakos 2001, HAT), the Northern Sky Variability Survey (Wozniak et al. 2004, NSVS), and ROTSE-I. Variable stars, notably Cepheids, RR Lyrae-type,  $\delta$  Scuti-type, SX Phonencis-type, semi-regular variables, and eclipsing binaries are shown to be ubiquitous in Galactic fields and in clusters. The next-generation projects like the cyclic all-sky survey by the Panoramic Sky Survey And Rapid Response System (Pan-STARRS) no doubt will provide a much complete variable star census and characterization to enhance vastly our understanding of the cosmos in the time domain.

While the main goal of the TAOS project is to conduct a KBO census by detecting stellar

occultations, the plethora of time-series stellar photometry renders the opportunity to identify and characterize variable stars spanning a wide range of timescales, from less than a second to a few years. The first paper of the series of the TAOS stellar variability studies deals with detection of low-amplitude  $\delta$  Scuti stars (Kim et al. 2009). The current paper, the second in the series, presents the effort to identify variable stars in a targeted star field.

## 2. Observations and Data Reduction

The TAOS telescope system consists of an array of four 50 cm, fast optics (f/1.9), wide-field robotic telescopes, sited at Lulin Observatory (longitude  $120^{\circ} 50' 28''$ E; latitude  $23^{\circ} 30'$  N, elevation 2850 meters) in central Taiwan. Each telescope is equipped with a  $2048 \times 2048$  SI-800 CCD camera, with a pixel scale of  $2.9''$ , yielding about a 3 square degree field of view on the sky. The TAOS system uses a broad custom-made filter which, together with the sensitivity of the CCD, has a response function close to that of a standard broad R-band filter.

All TAOS telescopes observe the same star field simultaneously so as to eliminate false detection of occultation events by KBOs. Each observing session begins with regular imaging (“*stare mode*”) of the star field, followed by a special CCD readout operation (“*zipper mode*”). In the zipper mode, the camera continues to read out a block of pixels at a time while the shutter remains open. A stellar occultation by a km-sized KBO is expected to last for only a fraction of a second, and it is this pause-and-shift charge transfer operation that allows 5 Hz photometric sampling to detect such an event. The zipper-mode data are most suitable to study truly fast varying phenomena such as stellar flaring, but they were not used in the results reported in this paper so will not be discussed further. Technical details of the TAOS operation can be found in Lehner et al. (2009).

The primary purpose of the stare-mode observations is to provide guidance of the pointing of the star field, particularly for photometric processing of the zipper-mode images, but the stare-mode data can be used also for stellar variability studies. A set of stare-mode observations consists of 9 telescope pointings, each with 3 frames of images, dithered around the center of target field. The frames covering the central position were used in the analysis reported here.

There are a total of 167 TAOS star fields, mostly along the ecliptic plane. These fields have been selected to have few exceedingly bright ( $R < 7$ ) stars, and to have a sufficient number of stars to maximize occultation probability, yet not too crowded to hamper accurate stellar photometry. The number of stars brighter than about  $R \sim 16$  ranges from a few hundreds to several thousands in each of our target fields.

This paper presents the variable stars found in a particular field, No. 151, which has the central coordinates  $RA = 17^{\text{h}}30^{\text{m}}6^{\text{s}}.67$ ,  $Dec = 27^{\circ}17'30''$ (J2000). After excluding data taken under inferior sky conditions, the data presented here include 93 good photometric measurements taken at 47 epochs from 2005 April 11 to 2005 August 02. Each photometric measurement came from a stare-mode image with a 4 s exposure.

Photometry was performed using the *SExtractor* package (Bertin & Arnouts 1996) with a  $3\sigma$  source detection limit. For each detected source, the output provides the x-y position, instrumental magnitude, magnitude error, FWHM, etc. Astrometry was done using *imwcs* task of *WCSTools*<sup>1</sup> (Mink 1999) with the USNO-B1.0 catalog (Monet et al. 2003). Then the CCD x-y positional output from the *SExtractor* was converted to sky coordinates (RA and DEC) for individual images using the *xy2sky* task of *WCSTools*.

The stellar position was matched with the USNO-B1.0 and 2MASS (Cutri et al. 2003) catalogs. The USNO-B1.0 catalog was derived from images of digitization of sky-survey photographic plates, and gives the position, proper motions, photographic magnitude in each of the five passbands (B1, B2, R1, R2, I), and star/galaxy estimators for some 1,042,618,261 objects. The 2MASS Point Source Catalog essentially covers the whole sky in three near-infrared bands J, H and  $K_s$ , down to a limiting magnitude of  $J \sim 15.8$  mag with a signal-to-noise ratio of 10. Optical magnitudes, USNO unique identification numbers (USNO ID), and 2MASS magnitudes of the detected sources in our images were obtained by matching the position to the USNO-B1.0 and 2MASS catalogs. A matching radius of  $10''$  was used, which gives unambiguous identifications in all but a few cases. The catalog for each image provides the unique USNO\_id, TAOS instrumental magnitude, optical magnitude (B2, R2), 2MASS\_id, and infrared (J, H,  $K_s$ ) magnitudes.

We then created the lightcurve for each star, containing the modified Julian date (MJD), calibrated TAOS magnitude, and error in magnitude. Photometric calibration of the TAOS instrumental magnitude will be discussed in the next section. Only data with good photometric quality, judged on the basis of the number of detected sources, were used in the analysis. Best images are those with more than 3000 detected sources. In the results reported here, we only considered images having more than 2500 detected sources. For variability analysis, only sources with more than 80 photometric measurements were considered. Finally we had the lightcurves of 2915 sources, mostly with 93 photometric measurements.

## 2.1. Photometric Calibration

TAOS images are obtained with a filter close (but not identical) to the standard R optical band. We used the R2 magnitude in the USNO-B1.0 catalog to calibrate our TAOS instrumental magnitude with a linear fit, under the assumption that most stars are not variable. Despite the large photometric scattering intrinsic to the USNO-B1.0 catalog (derived from photographic plates), the calibration gives a consistent rescaling of the TAOS instrumental magnitude for each star so as to remove run-to-run variable sky transparency, atmospheric extinction due to different air-masses, and telescope system variations. One such calibration curve for a particular image is shown in Figure 1.

---

<sup>1</sup>Package available at <http://tdc-www.harvard.edu/software/wcstools/>

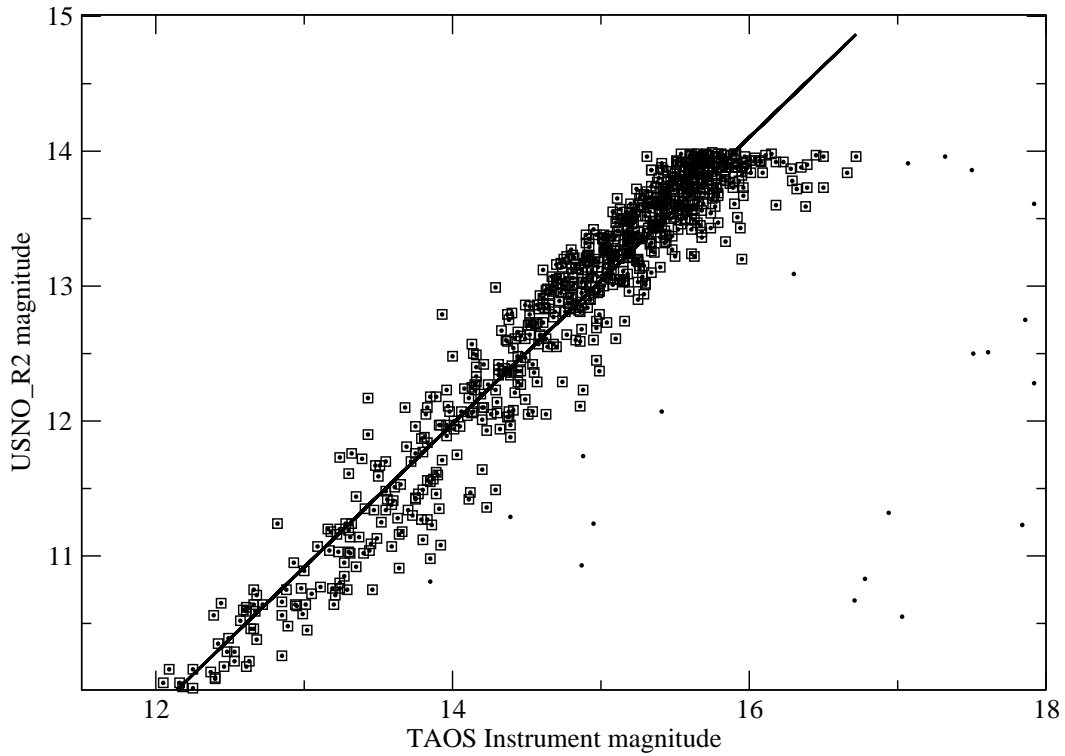


Fig. 1.— The TAOS instrument magnitude versus the R2 magnitude in the USNO-B1.0 catalog. The dots shows all the TAOS measurements, whereas the squares mark those stars with a corresponding R2 magnitude between 10 and 14 used in the linear fitting, shown as the solid line. Outliers, i.e., TAOS detections with mismatched USNO magnitudes, are caused by the photometric scattering of the USNO-B1.0 photometry or bad pixels in the TAOS images.

## 2.2. Periodicity Analysis

We used the *Lomb-Scargle* (LS) periodogram (Lomb 1976; Scargle 1982) to determine the most likely period of a variable star. The LS method computes the Fourier power over an ensemble of frequencies, and finds significant periodicities even for unevenly sampled data. We used the algorithm taken from the Starlink<sup>2</sup> software database available publicly, and verified the periods further with the software *Period04*<sup>3</sup> (Lenz & Breger 2005) for stars displaying obvious periodic variation. *Period04* also provides the semi-amplitude of the variability in a lightcurve. For any star showing a possibly spurious period, we carefully checked the phased lightcurve for that particular period.

## 3. Results

### 3.1. Candidate Variables

Because a large number of stars have been observed, the random errors of the differential magnitudes are well determined. These amount to  $\sim 0.02$  mag at TAOS magnitude  $\lesssim 14$  but increases to  $\sim 0.1$  mag at  $\sim 16$  mag. To illustrate this, Figure 2 shows the lightcurves of a few nonvariable stars (per our analysis) as well as known variable stars. Figure 3 shows the variations of the lightcurves of 2900 stars in the selected field. Each point represents the root-mean-square (RMS) of 80–93 measurements of a particular star over 105 days. One sees that most stars behave “normally”, i.e., the signal to noise decreases for fainter stars, as expected. The increase of RMS at the bright end ( $< 8$  mag) is due to saturation. An outlier, that is, a star with a large RMS value for its magnitude, is then considered a likely variable.

A total of 143 variable star candidates were identified on the basis of  $3\sigma$  above the average RMS in a magnitude bin. Visual inspection of the lightcurves indicated that 62 stars show large RMS values because of flux drops of only a few data points, e.g., as the result of bad pixels or cosmic rays. These were excluded from the variable list. At the end we had the final count of 81 candidate variables.

### 3.2. Previously Known Variables

We have searched the *International Variable Star Index* (VSX)<sup>4</sup> of the American Association of Variable Star Observers (AAVSO) for known variables in our field. The VSX database

---

<sup>2</sup><http://www.starlink.uk>

<sup>3</sup><http://www.univie.ac.at/tops/Period04>

<sup>4</sup><http://www.aavso.org/vsx/>

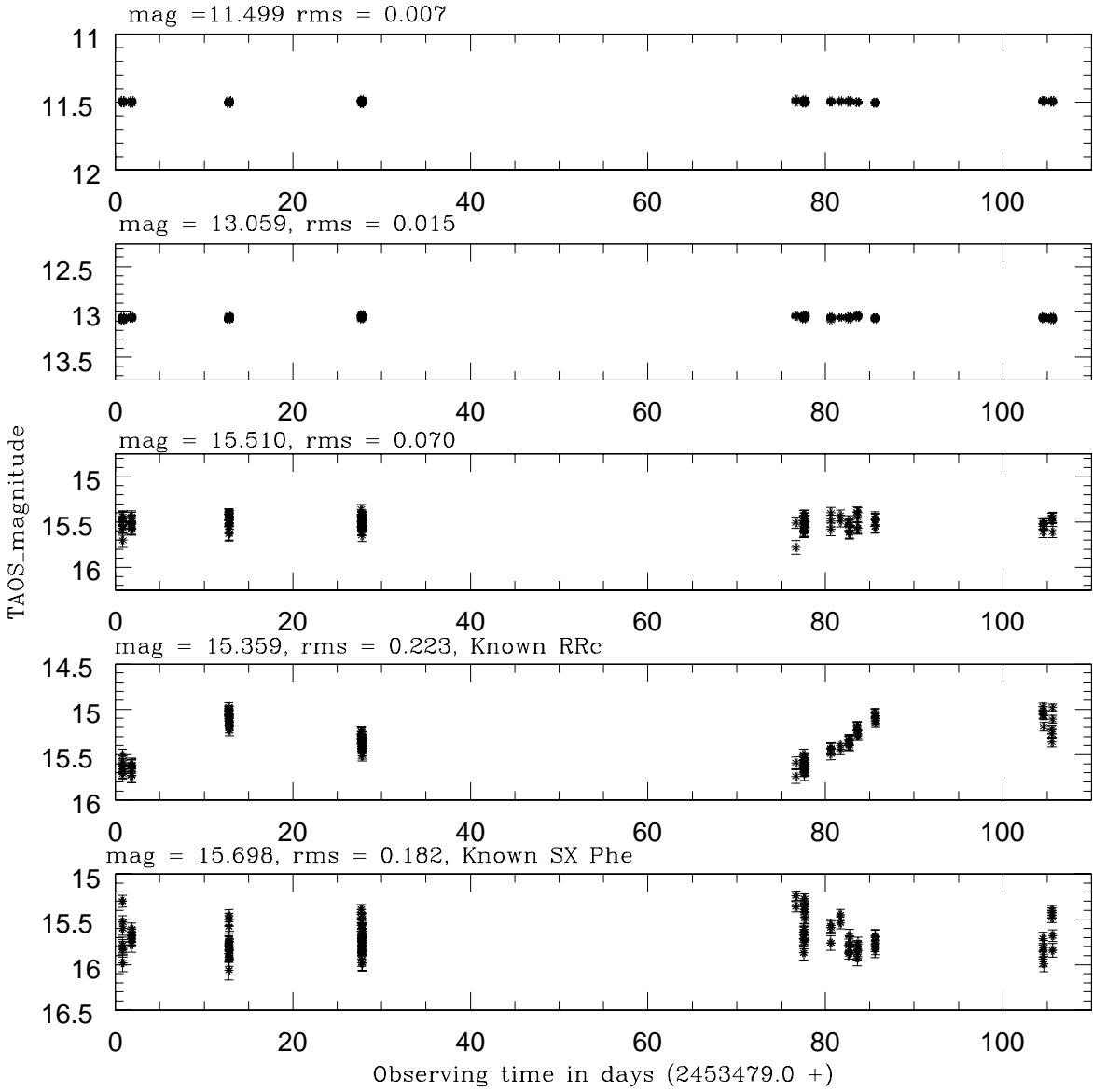


Fig. 2.— Example lightcurves of a few apparently nonvariable stars (top 3 panels) and known variable stars.

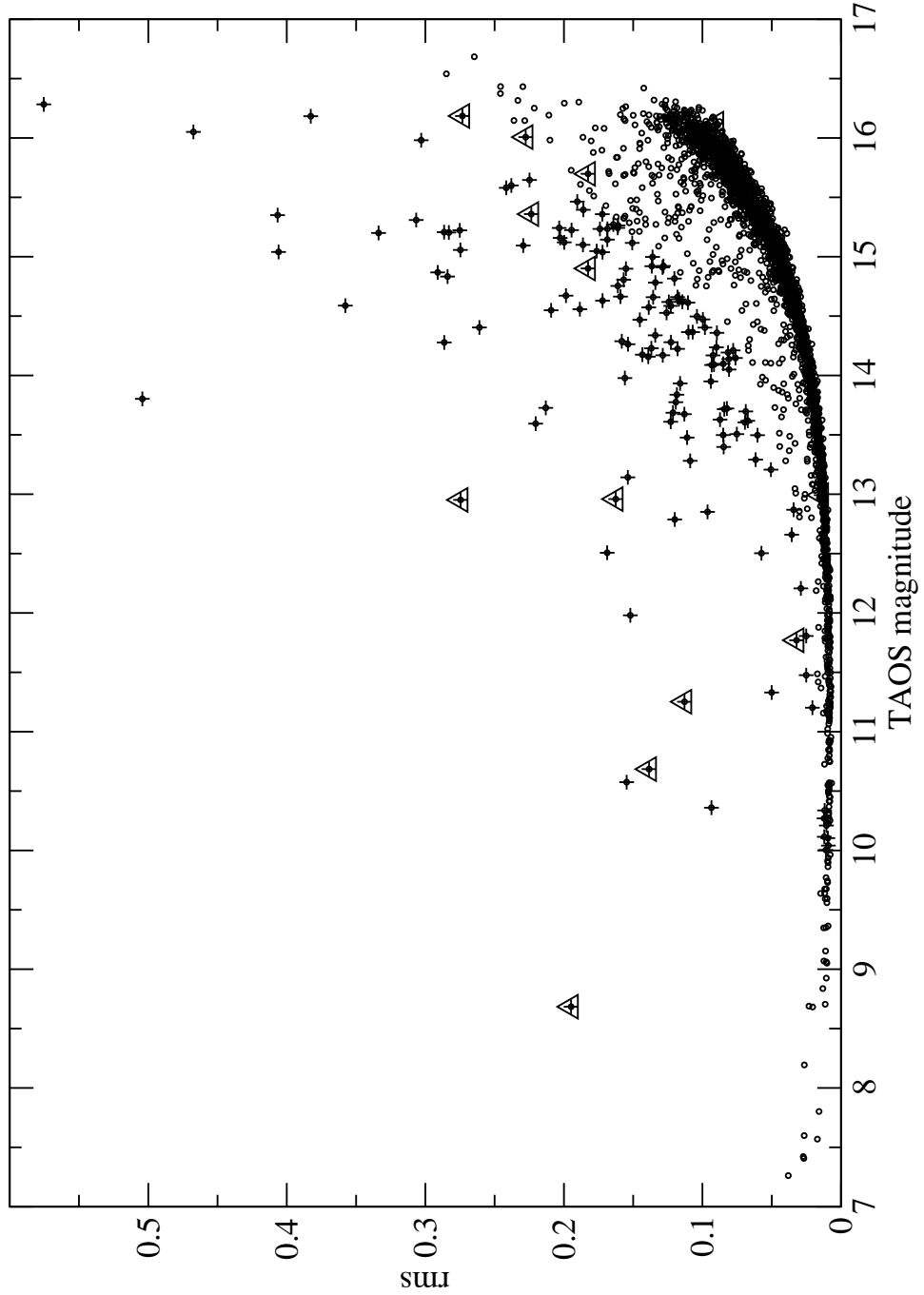


Fig. 3.— The root-mean square of the magnitudes of some 2900 stars in the  $2.9 \text{ deg}^2$  field of the TAOS Field 151 (RA =  $17^{\text{h}}30^{\text{m}}6^{\text{s}}.67$ , Dec =  $27^{\circ}17'30''$ ). Each dot represents the RMS of the lightcurve of each of the 2900 stars in the field. The triangles mark known variables. The plus symbols tag the sources having more than  $3\sigma$  variability in the lightcurves, hence are variable light



is populated with the *General Catalogue of Variable Stars* (GCVS) (Khopolov et al. 1998), the New Catalog of Suspected Variable Stars (Kukarkin et al. 1982), and the published data from sky surveys, e.g., the Northern Sky Variability Survey (NSVS) (Wozniak et al. 2004), the All Sky Automated Survey (ASAS) (Pojamanski, Pilecki & Szczygiel 2005), and the Optical Gravitational Lensing Experiment-phase 2 (OGLE-II) (Wozniak et al. 2002).

A total of 19 variables from the VSX database are found in our field, and we recovered 14 of them, listed in Table 1. Missing objects in our list of known variables include one star that is brighter than our saturation limit so was not included in our analysis. Two stars, namely ASAS J172907+2749.4 (Pojamanski 2002) and ROTSE1 J172907.35+274928.6 (Akerlof et al. 2000), with a  $3.6''$  coordinate difference, are classified as an RRAB with similar periods. They should be the same star, and we recovered the object as USNO-B1 ID 1178.0358793 with a similar period. Another two entries in the VSX, namely ROTSE1 J173203.69+272225.1 from ROTSE-I data (Akerlof et al. 2000) and ASAS J17320+2722.4 from HAT data (Pojamanski 2002), also with a  $3.6''$  difference in the published coordinates, have only one counterpart in our data as USNO-B1 ID 1173.0334705. They are detected as one star by the TAOS telescope system, which has a large  $3''$  pixel scale. We suspect the  $3.6''$  coordinate difference to be a systematic offset in the ASAS catalog, and these two entries actually refer to the same star. This star is classified as a long-period variable (LPV) by ROTSE-I without period determination. We estimated the period to be about 104 days.

Of the three stars, V0486 Her, ROTSE1 J172638.42+265616.5 and ASAS J172638+2656.3, the first two having the same coordinates, period (0.8059/0.8056 days) and classification (RRAB), but as separate entries in the VSX database. The third star, again  $3.6''$  away, should also be the same star, though ASAS gave a similar brightness but classified it as a CW-FU with a different period (4.203 days). We recovered one variable as USNO ID 1169.0316280 in the position, with a period of 0.8061 days. We hence caution on the possible multiple entries of the same variable star in the VSX database.

The VSX database provides information on the variable type, period, and magnitude range. Table 1 lists the period and semi-amplitude of known variables derived from our new data, together with VSX information. The first two columns are the star name and the USNO identification number (ID). The third and fourth columns provide the visual magnitude range in the VSX database and our TAOS magnitude range. Columns 5 to 7 give, respectively, the number of observed frames, RMS in TAOS magnitude and the variable classification from the VSX database (such as the pulsating types of LB and LPV, RRAB, and RRC, and the eclipsing binary types of EW and EA, and the  $\delta$  Scuti type of SX Phe.) Column 8 provides the period taken from the VSX catalog, while the ninth and tenth columns give the periods we derived using the LS method and *Period04*, described in Section 2.2. Column 11 provides the semi-amplitude determined by *Period04*. The star NT Her is a known LB variable, but without a published period. Our data suggest a long period,  $\sim 74$  days with a large uncertainty. For the rest of known variables, the periods we determined are consistent, except in harmonics in some cases, with those listed in the VSX. The lightcurves of the 14 previously known variable stars are shown in Figure 4.

Table 1. Known Variable Stars

USNO id	Star Name	Vmag	Tmag	Frames	$\sigma_T$	Type	P <sub>known</sub>	P <sub>LS</sub>	Period04	Semiamp
1178.0360412	NT Her	10.0-10.6	8.33- 8.96	90	0.192	LB	NA	74.5240	74.8600	0.309
1169.0319910	V1097 Her	10.7-11.3	10.51-11.00	88	0.133	EW	0.3608	0.1804	0.1805	0.179
1173.0334705	ASAS J173204+2722.4 ROTSE1 J173203.69+272225.1	11.51(0.336)	11.10-11.40	93	0.113	MISC LPV	-	~ 104	~ 104	0.19
1177.0363083	V1060 Her	12.1-12.8	11.72-11.90	92	0.032	EA	1.5768	0.7012	1.5873	0.220
1169.0316280	V0486 Her ROTSE1 J172638.42+265616.5	12.8-13.6 13.551(0.497)R1	12.70-13.25	89	0.161	RRAB RRAB	0.8059 0.8056	0.8061	0.8059	0.190
1178.0358793	ASAS J172638+2656.3 ASAS J172907+2749.4 ROTSE1 J172907.35+274928.6	12.769(1.202) 12.406(0.785) 12.85-13.50(R1)	12.43-13.31	93	0.274	CW-FU RRAB RRAB	4.203 0.46883 0.46885	0.469	0.48871	0.310
1171.0322166	1RXS J172719.4+270858	12.9(0.12)	12.96-13.03	93	0.0143	UV	-	0.7486	0.7489	0.011
1174.0340307	V0420 Her	14.5-15.6	14.37-15.18	86	0.179	RRAB	0.6003	0.7464	0.5997	0.220
1179.0338666	[WM2007] 772	15.29(0.17)	14.99-15.27	93	0.053	VAR	-	0.1061	0.1107	0.026
1167.0305285	V0413 Her	15.6-16.3	14.97-15.74	90	0.223	RRC	0.5137	0.5131	0.5126	0.271
1180.0314388	V0879 Her	15.2-15.8	15.24-16.06	82	0.175	SXPhe	0.0569	0.0569	0.0538	0.193
1179.0338257	[WM2007] 771	16.28(0.18)	15.94-16.36	67	0.091	VAR	-	0.9682	1.0172	0.04
1169.0316908	V0404 Her	16.0-16.8	15.51-16.57	72	0.2276	RR	0.55509	0.20918	0.6616	0.195
1169.0316979	V0405 Her	15.8-17.0	15.76-16.79	47	0.2733	RRAB	0.5879	0.5880	1.4287	0.296

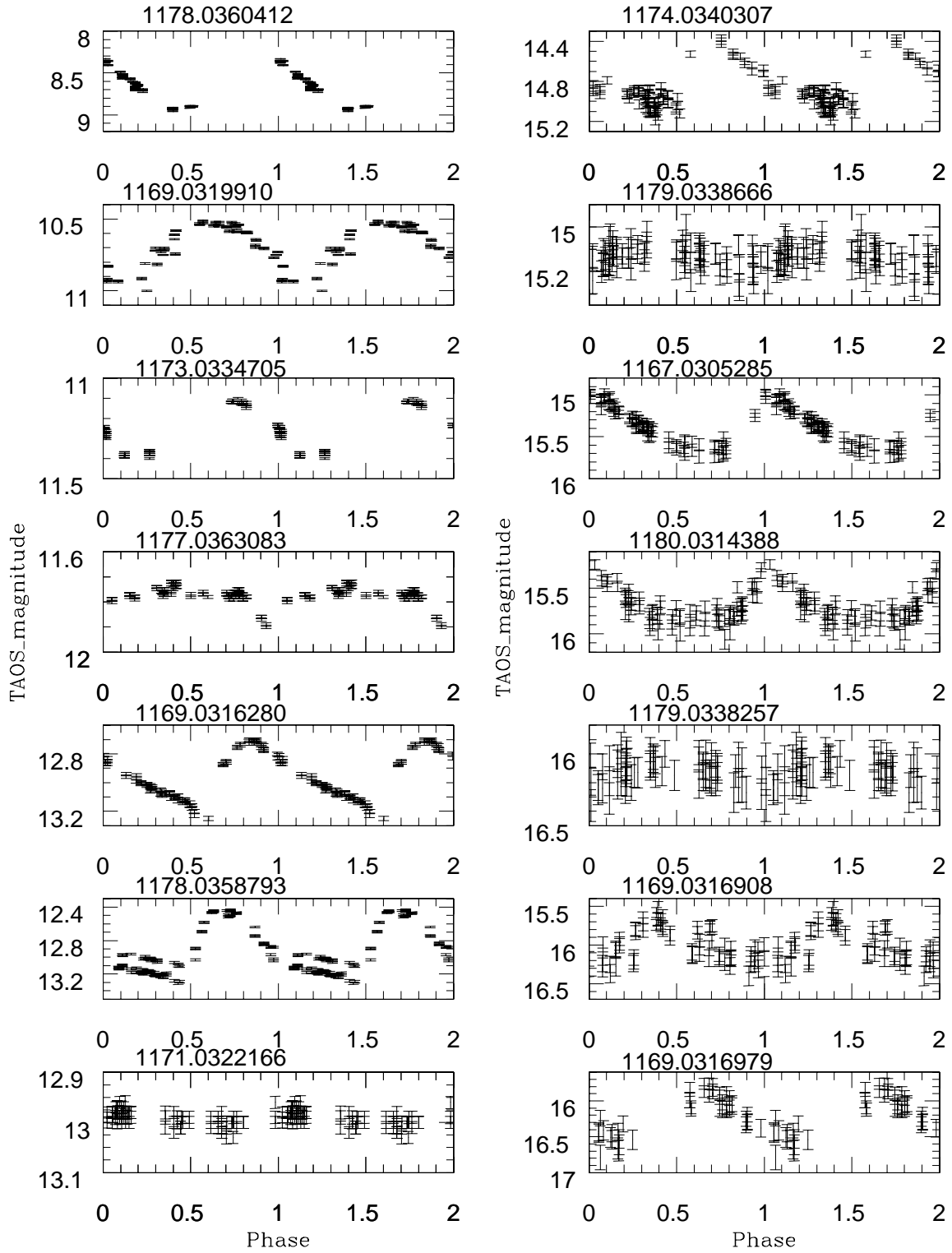


Fig. 4.— Phased lightcurves of known variables in Table 1.

### 3.3. Newly Found Variables

Of the 67 previously uncatalogued variable candidates, 15 stars show clearly perceived phased lightcurve patterns with periods well determined by the LS algorithm. Periods derived from the two LS methods generally matched well. The remaining 52 candidates either did not show any significant periods, perhaps because of insufficient phase coverage of our data, or the phased lightcurves did not show patterns readily recognizable. Table 2 summarizes the properties of the 15 newly found variables. The first four columns are the TAOS star identifier, RA and DEC coordinates taken from the USNO-B1.0 catalog, both in degrees, and the ID in the USNO catalog. Columns 5 and 6 give the calibrated TAOS magnitude and its error. The 7th and 8th columns are the magnitude RMS of the lightcurve and the number of observations used in the analysis. Column 9 is the derived period and column 10 gives the variable classification on the basis of the shape of lightcurves, periods, and semi-amplitudes.

The phased lightcurves of the 15 classified variables are shown in Figure 5. Among these, 4 are RR Lyrae (RR) variables, 3 are semi-regular (SR) variables, 5 are broadly classified as eclipsing binaries (EW), and one each has been classified as a  $\delta$  Scuti (Dset), Cepheid (Cep) or SX Phonencis (SX Phe) variable.

Cepheids (Cep) are massive stars with a spectral class of F at maximum light while G to K at minimum; they generally have periods in the range of 1–70 days with an amplitude variation of 0.1 to 2.0 mag in V. RR Lyrae-type (RR) stars are radially pulsating giants with a spectral class A–F; they have periods of 0.2 to 2.0 days with an amplitude variation of 0.3 to 2.0 mag in V. The  $\delta$  Scuti-type variable stars are A3-F0 main-sequence or sub-giant stars located in the lower part of the classical instability strip in the H-R diagram, with short pulsating periods ranging from 0.02 to 0.3 days and amplitudes less than 0.1 mag in V. The SX Phonencis (SX Phe) stars are pulsating sub-dwarfs with a spectral type A2–F5. Their light variations resemble those of  $\delta$  Scuti variables, but with shorter periods, 0.04 to 0.08 days, and larger magnitude variations, up to 0.7 mag in V. Semiregular (SR) variable are generally giants or supergiants of intermediate or late (K-M) spectral types. SRs show noticeable periodicity in their lightcurves, with periods in the range from 20 to 1000 days and amplitudes varying in the range from 0.1 to 2.0 mag in V. Eclipsing binaries are binary systems with the orbital plane lying near the line-of-sight of the observer.

Table 3 presents the USNO  $B, R2$  and 2MASS  $J, H, K_s$  magnitudes of the previously known variable stars and the variables found by our analysis, i.e., those listed in Table 1 and Table 2. In addition to lightcurves, the color information of the stars could be used to cross-check the classification of variable stars. TAOS data do not provide color information, so we used the 2MASS data (Cutri et al. 2003) for this purpose. The 2MASS observations were taken simultaneously in the  $J, H,$  and  $K_s$  bands, thus the colors  $(J - H)$  and  $(H - K_s)$  are sampled at the same phase of a variable’s light cycle. The near-infrared colors of RRab stars are in the range  $(J - H) = -0.1$  to 0.5 mag and  $(H - K_s) = -0.1$  to 0.25 mag (Kinemuchi et al. 2006). Figure 6 displays the 2MASS colors of the variable stars listed in Table 3, along with the loci of dwarfs, giants

Table 2. Previously unknown variables

ID	RA (J2000) [Deg.]	DEC (J2000) [Deg.]	USNO ID	TAOS_mag [mag]	mag_err [mag]	RMS [mag]	Frame No	Period (days)	Classification
TAOS 151-01	262.0523250	+27.2035170	1172.0333288	11.330	0.005	0.0501	93	22.065	SR1
TAOS 151-02	261.7864306	+27.0041889	1170.0320366	11.806	0.007	0.0251	93	59.891	SR2
TAOS 151-03	262.5683400	+27.8393820	1178.0359464	12.503	0.009	0.0574	93	34.936	SR3
TAOS 151-04	261.6632700	+27.3628750	1173.0332057	12.659	0.010	0.0356	92	2.409	Cep
TAOS 151-05	263.3984850	+27.6555000	1176.0347892	12.869	0.011	0.0342	93	0.439	RR1
TAOS 151-06	262.7197200	+27.6675860	1176.0346875	13.498	0.016	0.0850	92	0.147	SXPhe
TAOS 151-07	262.3019550	+27.6931360	1176.0346036	13.722	0.019	0.0823	93	0.280	EW1
TAOS 151-08	261.9320400	+27.6780570	1176.0345244	14.088	0.023	0.0934	93	0.622	RR2
TAOS 151-09	263.3462100	+26.7278840	1167.0306057	14.497	0.031	0.1040	93	0.401	RR3
TAOS 151-10	262.6746600	+26.4792490	1164.0287321	14.619	0.033	0.1243	93	0.264	Dsct
TAOS 151-11	263.1983550	+27.1243050	1171.0324737	14.672	0.035	0.1985	93	0.174	EW2
TAOS 151-12	262.9039200	+26.4763810	1164.0287687	15.121	0.048	0.1998	87	0.264	EW3
TAOS 151-13	262.8258600	+26.4790000	1164.0287567	15.158	0.049	0.2028	93	0.264	EW4
TAOS 151-14	263.4367250	+26.5488583	1165.0285251	15.235	0.052	0.1686	84	0.430	EW5
TAOS 151-15	263.2523100	+27.1410000	1171.0324817	15.680	0.171	0.156	93	0.621	RR4

and supergiants (Bessell & Brett 1998) for reference. With a few exceptions, the location of each variable is reasonably positioned in the color-color diagram according to its class.

#### 4. Summary and future work

We have identified a total of 81 candidate variable stars in a particular field, No.151 (RA =  $17^{\text{h}}30^{\text{m}}6^{\text{s}}.67$ , Dec =  $27^{\circ}17'30''$ , J2000) in the TAOS survey. Among these, 29 variables can be classified, including 15 previously uncatalogued, as Cepheids, RR Lyrae stars, semiregular variables, eclipsing binaries or  $\delta$  Scuti-type variables. Their lightcurves, derived periods, semi-amplitudes, and hence the variable classification are presented here and the data are available on the TAOS website, <http://taos.asiaa.sinica.edu.tw/demo>. With the same methodology we expect to produce variable star lists in other TAOS fields, now with observations covering more than 4 years (2005–2009). In addition to stare-mode photometry, the zipper-mode observations provide data sampled at 5 Hz, so may be particularly useful for fast stellar variability (Kim et al. 2009). The TAOS database hence has the unique potential to study several thousand stars at timescales from less than a second to a few years.

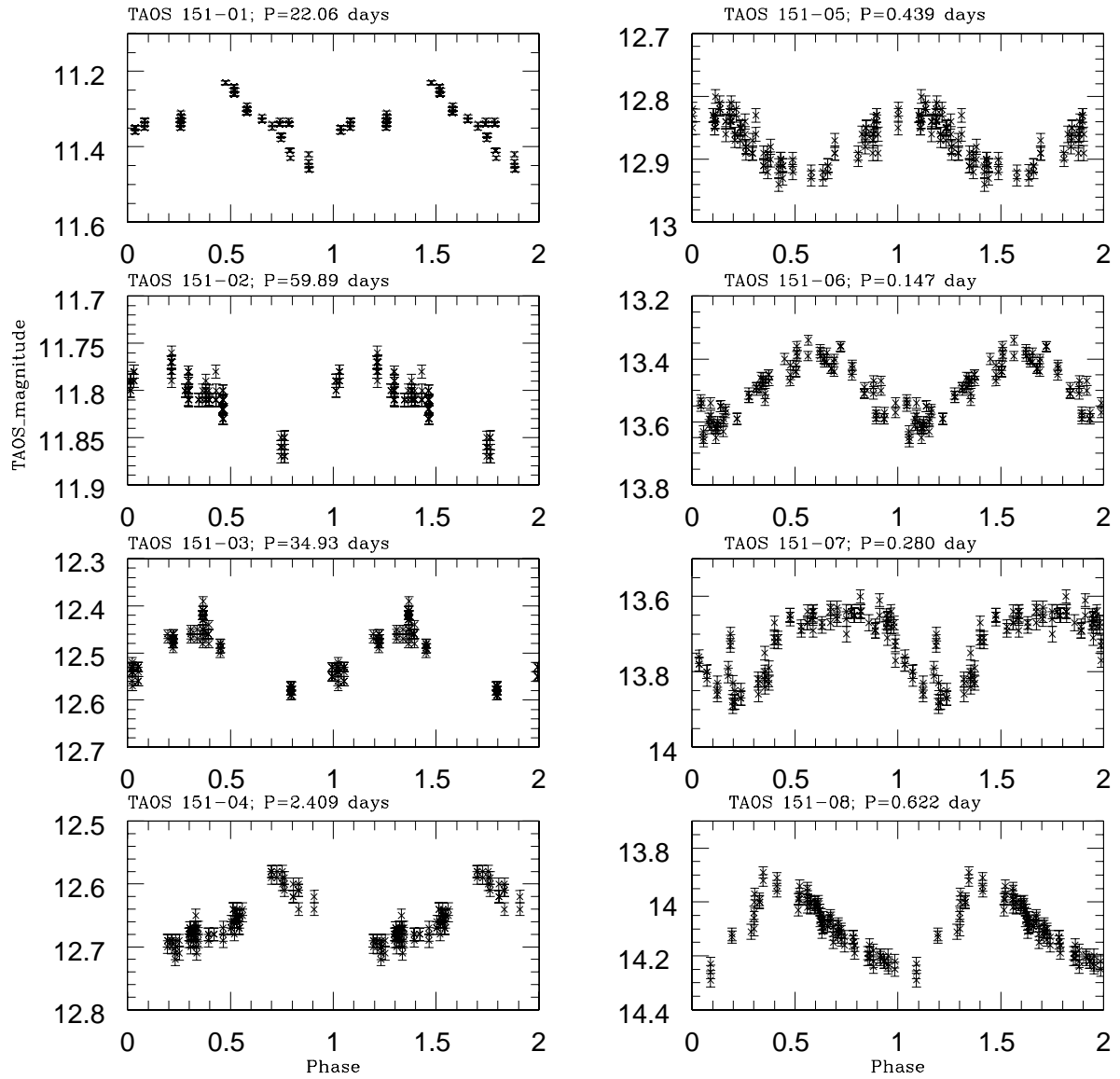
The work at National Central University was supported by the grant NSC 96-2112-M-008-024-MY3. YIB acknowledges the support of National Research Foundation of Korea through Grant 2009-0075376. Work at Academia Sinica was supported in part by the thematic research program AS-88-TP-A02. Work at the Harvard College Observatory was supported in part by the National Science Foundation under grant AST-0501681 and by NASA under grant NNG04G113G. SLM's work was performed under the auspices of the U.S. Department of Energy by Lawrence Livermore National Laboratory in part under Contract W-7405-Eng-48 and by Stanford Linear Accelerator Center under Contract DE-AC02-76SF00515. KHC's work was performed under the auspices of the U.S. Department of Energy by Lawrence Livermore National Laboratory in part under Contract W-7405-Eng-48 and in part under Contract DE-AC52-07NA27344.

#### REFERENCES

- Akerlof, C. et al.(2000, AJ, 119, 1901  
Alcock, C., et al. 1995, AJ, 109, 1653  
Alcock, C., et al. 1998, AJ, 115, 1921  
Alcock, C., et al. 2003, Earth, Moon & Planet, 92, 459  
Axelrod, T. S. et al. 1992, in ASP Conf. Ser. 34, Robotic Telescopes in the 1990s, Ed. A. V. Filippenko (San Francisco: ASP), 171

Table 3. Catalog for variable stars

USNO ID	$\Delta$ diff (")	USNOB2 [mag]	USNOR2 [mag]	J [mag]	H [mag]	$K_s$ [mag]
Known variables						
1178.0360412	0.252	10.18	8.61	4.640	3.650	3.171
1169.0319910	0.540	11.38	10.64	9.889	9.591	9.510
1173.0334705	0.072	12.53	11.24	9.150	8.497	8.342
1177.0363083	0.432	12.54	11.49	10.431	9.933	9.779
1169.0316280	0.576	13.72	13.20	11.970	11.760	11.715
1178.0358793	0.504	14.08	12.61	12.398	12.124	12.115
1171.0322166	0.252	14.77	12.60	9.796	9.213	8.970
1174.0340307	0.972	15.32	15.16	13.799	13.561	13.549
1179.0338666	0.324	15.80	14.85	14.165	13.906	13.861
1167.0305285	0.900	.....	15.00	14.681	14.420	14.159
1180.0314388	0.396	15.91	15.72	14.969	14.774	14.801
1179.0338257	0.720	16.95	15.90	15.094	14.713	14.683
1169.0316908	0.288	16.32	15.74	15.359	15.126	15.155
1169.0316979	0.396	16.44	16.10	15.299	15.133	15.039
Unknown variables						
1172.0333288	0.864	12.64	11.02	8.264	7.392	7.129
1170.0320366	0.828	14.47	11.24	10.491	9.901	9.852
1178.0359464	0.540	14.61	12.64	9.097	8.221	7.947
1173.0332057	0.180	13.63	12.83	11.360	10.852	10.715
1176.0347892	0.756	13.18	12.11	11.830	11.486	11.416
1176.0346875	0.648	14.12	13.25	12.211	11.731	11.632
1176.0346036	0.468	14.69	13.91	12.796	12.479	12.406
1176.0345244	0.612	15.19	14.12	13.134	12.902	12.835
1167.0306057	1.440	15.01	14.59	14.071	13.906	13.840
1164.0287321	0.252	15.96	14.92	13.404	12.843	12.747
1171.0324737	0.252	15.43	14.86	13.428	13.063	13.039
1164.0287687	0.468	17.31	15.46	13.453	12.824	12.594
1164.0287567	0.180	16.56	15.64	14.701	14.319	14.343
1165.0285251	7.056	20.09	18.65	16.687	16.198	15.663
1171.0324817	0.684	16.31	15.88	14.738	14.372	14.403





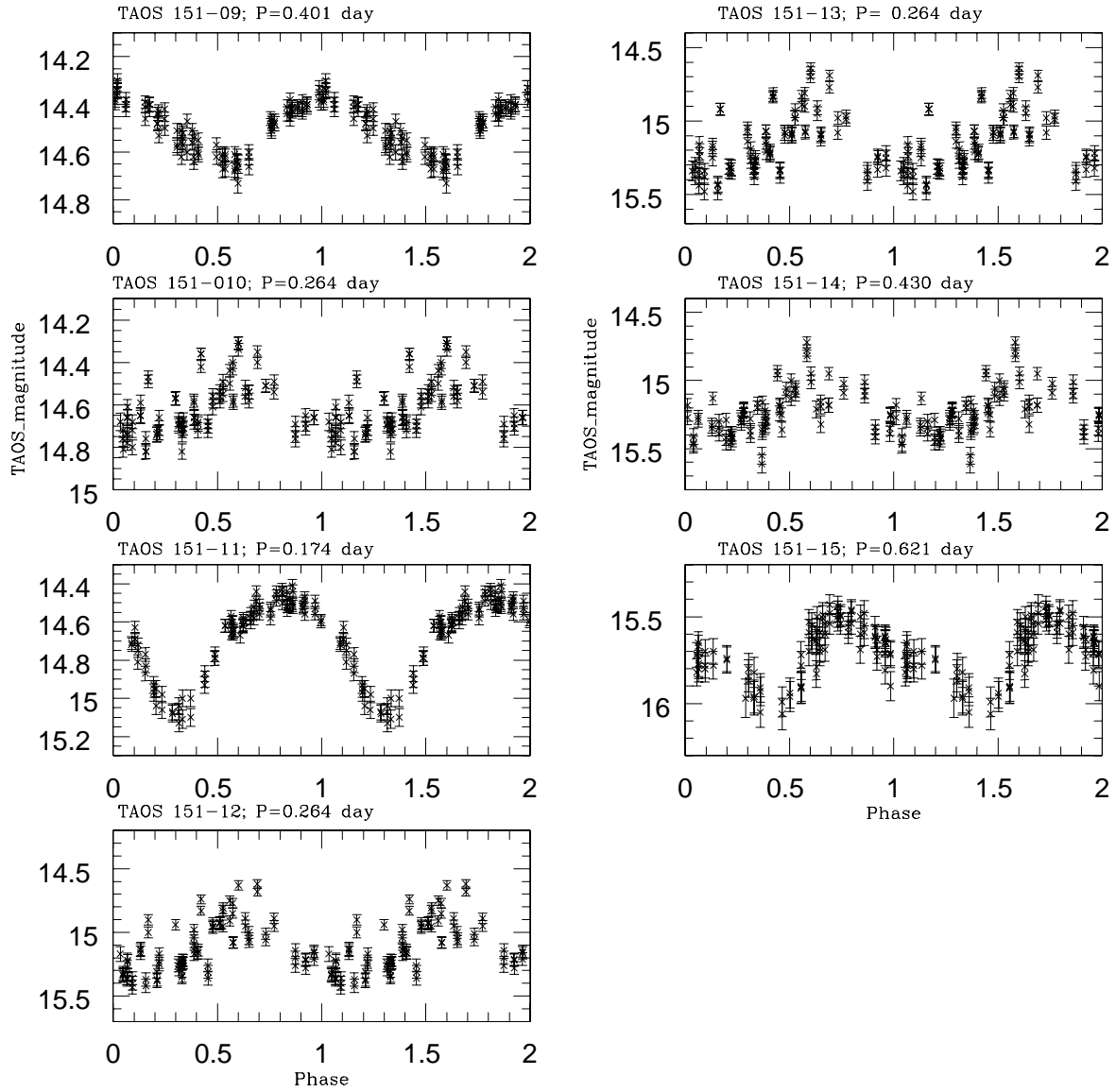


Fig. 5.— Phased lightcurves of newly identified variables with the TAOS data.

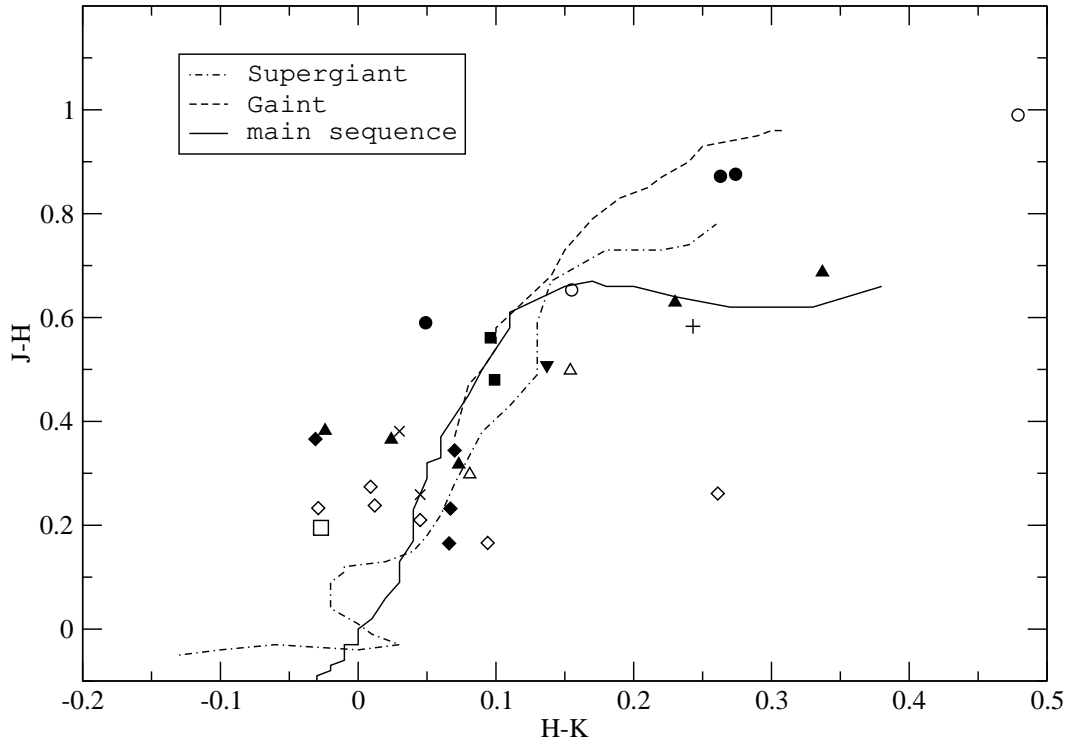


Fig. 6.— The 2MASS (J-H) versus (H-K<sub>s</sub>) colors of variables stars. The loci of dwarfs, giants and supergiants are taken from Bessell & Brett (1998). The open and filled symbols represent previously known and newly found variables. Different symbols are for various variable classes: circles for SR, LPV, LB, diamonds for RRAB, RRC, upward triangles for EW, EA, squares for SX Phe, DSct, downward triangles for Cep, pluses for UV, and crosses for VAR.

- Bakos, G. 2001, Pub. Astron. Dept. Eötvös Univ., 11, 107 or  
<http://www.cfa.harvard.edu/~gbakos/HAT>
- Beaulieu, J.P., et al. 1995, A&A, 303, 137
- Bailey, M. E. 1976, Nature, 259, 290
- Bernstein, G. M., Trilling, D. E., Allen, R. L., Brown, M. E., Holman, M. & Malhotra, R. 2004, ApJ, 128, 1364
- Bertin, E., & Arnouts, S. 1996, A&AS, 117, 393
- Bessell, M.S. & Brett, J.M., 1998, PASP, 100, 1134
- Bianco, F. B. et al. submitted to AJ
- Cieslinski, D. et al. 2003, PASP, 115, 193
- Cutri, R. M., et al. 2003, 2MASS All Sky Catalog of Point Sources (Pasadena:IPAC)
- Derue, F. et al. 2002, A&A, 389, 149
- Dyson, F. J. 1992, QJRAS, 33, 45
- Edgeworth K. E. 1949, MNRAS, 109, 600
- Hoffman D. I., Harrison T. E., McNamara B. J., 2009, AJ, 138, 466
- Kholopov, P. N., et al. 1998, Combined General Catalogue of Variable Stars, GCVS, SIMBAD
- Kim, D.-W. et al. 2009. AJ, 139, 757
- King, S. K. 2001, in *Small-Telescope Astronomy on Global Scales*, eds. W. P. Chen, C. Lemme, & B. Paczynski, ASP Conf. Ser, 246, 253
- Kinemuchi, K., Smith, H.A., Woźniak, P.R. & Mckay, T.A., 2006, AJ, 132, 1202
- Kuiper G. P., 1951, in *Astrophysics*, ed. J. A. Hynek, p.357 (McGraw-Hill, New York)
- Kukarkin B.V., et al. 1982, *New Catalogue of Suspected Variable Stars*, Nauka, Moscow
- Lehner, M. J. et al. 2006, Astron. Nach., 327, 814
- Lehner, M. J., et al. 2009, PASP, 121, 138
- Lenz, P. & Breger, M. *Comm. Asteroseismol.*, 146,53
- Lomb, N.R. 1976, Ap&SS, 39, 447

- Mink, D. J. 1999, in in ASP Conf. Ser. 172, *Astronomical Data Analysis Software and Systems VIII*, Eds. Mehringer, D. M., Plante, R. L. & Roberts, D. A. (San Francisco: ASP) 498
- Monet, D.G., et al. 2003, *AJ*, 125, 984
- Morbidelli A. & Levison H. F. 2003, *Nature*, 422, 30
- Pojamanski, G. 2002, *Acta Astron.*, 52, 397
- Pojamanski, G., Pilecki, B. & Szczygiel, D. 2005, *Acta Astron.*, 55, 275
- Scargle, J.D. 1982, *ApJ*, 263, 835
- Trujillo, C. A., Jewitt, D. C. & Luu, J. X. 2001, *AJ*, 122, 457
- Wozniak, P. R., et al. 2002, *Acta Astron.*, 52, 129
- Wozniak, P. R. et al., 2004, *AJ*, 127, 2436
- Wray, J.J. & Paczynski, B. 2004, *MNRAS*, 349, 1059
- Zhang, Z. W., et al. 2008, *ApJ*, 685, L157